Materials Advances

ROYAL SOCIETY OF CHEMISTRY

COMMUNICATION

View Article Online
View Journal | View Issue

Check for updates

Cite this: *Mater. Adv.*, 2020, 1, 2707

Received 5th August 2020,
Accepted 13th September 2020

DOI: 10.1039/d0ma00568a

rsc.li/materials-advances

Green synthesis of upconversion nanocrystals by adjusting local precursor supersaturation under aqueous conditions†

Su Li,[a] Jie Chen,[b] Yu Ying Tang,[a] Lin Yu Hu,[a] Wen Hui Qian,[a] Dong Zhu *[ab] and Peng Chen *[b]

We describe a green synthesis of upconversion nanocrystals (UCNs) by adjusting local precursor supersaturation under aqueous conditions at low temperature with size and phase control as well as high production yield. The synthesis allows the separation of nucleation and growth, leading to the formation of small UCNs with a uniform size. Ultra-small α-phase UCNs (~6.3 nm) and bright β-phase UCNs (~25.5 nm) have been synthesized.

Upconversion nanocrystals (UCNs) have wide-spread applications in imaging and sensing,[1–4] solar cells,[5] displays,[6] encryption[7,8] and photothermal therapy[9] because of their charming features including multicolored emissions, excellent photostability, and the capability to be excited by near-infrared (NIR).[10] The last feature is particularly beneficial for phototheranostics due to reduced auto-fluorescence, tissue damage and enhanced penetration depth.[11] $NaYF_4$:Yb^{3+},Tm^{3+} nanocrystals are paid special attention, not only because $NaYF_4$ is an efficient host material for upconversion emission,[12] but also because its excitation at 980 nm and upconversion emission around 800 nm are within the spectral scope recognized as the 'window of optical transparency' for biological tissues.[13]

Current synthesis methods for UCNs, however, usually suffer from the requirements for high temperature in the presence of high-boiling point organic solvents, long reaction time, surfactants, expensive and unstable precursors, or tedious procedures. These syntheses often are of low-yield and high-cost, and produce environmental hazards. The biological applications demand small-sized UCNs (<10 nm) to ensure thorough and fast clearance from the body.[14–19] But synthesis of ultra-small and uniform UCNs remains as a great difficulty. Synthesis of bright NIR-emitting UCNs for *in vivo* imaging is also challenging. UCNs may exist in either cubic (α) or hexagonal (β) phase. The α phase is metastable whilst the β phase, which gives enhanced UC emission, is thermodynamically stable. Transition from α to β phase, however, demands high reaction temperature of 300–320 °C in organic solvent and prolonged reaction time (even up to several days).[20–29]

In this contribution, we have developed a green strategy by adjusting local precursor supersaturation to synthesize uniform UCNs with high yield under mild aqueous conditions. The use of fatty acids as the chelating ligands for rare earth ions and as a stabilizer for UCNs reduces the energy barrier for nucleation and transition from α to β phase. Through rational designs, ultra-small α-UCNs (<7 nm) and bright β-UCNs (~25 nm) emitting at 800 nm are obtained.

For current synthesis methods, constant nuleation occurs concomitantly with nanocrystal growth because the reaction has to start with a concentration higher than needed for growth in order to initiate nucleation.[29] Some hydrothermal syntheses also provide a liquid nucleation model[30] or liquid–solid-solution phase transfer strategy.[31] Consequently, the produced nanoparticles are highly heterogeneous in size. To tackle this dilemma, we developed a strategy by adjusting the local precursor supersaturation to synthesize $NaYF_4$:Yb^{3+},Tm^{3+} nanocrystals as shown in Fig. 1.

Sodium oleate molecules (18 carbon fatty acid) were firstly diserpsed in aqueous solution. When rare earth (RE) ions are added with much lower abundance as compared to oleate, they are completely chelated by the carboxyl groups on the oleate molecules leading to the formation of aggregates ~1000 nm in size (Fig. S2 in the ESI†) because of charge neutralization. As a consequence, the local concentration of RE ions at the interface between aggregates is increased to exceed S_n (whereby it reduces ΔG_v). The subsequent addition of F^- ions triggers the nucleation of UCNs while some oleate molecules remain on the surface to lower the surface energy (ΔG_s). The appearance of the two wide peaks in the X-ray diffraction (XRD) pattern corresponding to the 111 and 220 planes of α-phase nanocrystals indicates the formation of small nuclei of UCNs (Fig. S3a in the ESI†).

[a] *School of Pharmacy, Nanjing University of Chinese Medicine, Nanjing, Jiangsu 210023, P. R. China. E-mail: dongzhu@njucm.edu.cn*
[b] *School of Chemical and Biomedical Engineering, Nanyang Technological University, 637457, Singapore. E-mail: chenpeng@ntu.edu.sg*

† Electronic supplementary information (ESI) available. See DOI: 10.1039/d0ma00568a

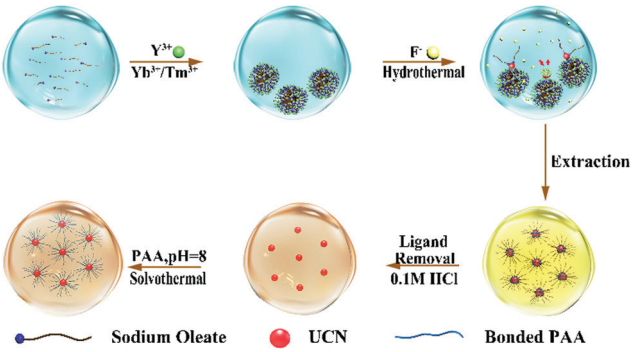

Fig. 1 Schematic illustration of green synthesis for UCNs.

Taken together, the nucleation process at the ambient temperature is favored in this system due to lowered ΔG even when the bulk concentrations of the precursor ions are low. At an increased temperature (120 °C), the growth of UCNs occurs at the aggregate interface and is sustained by surrounding chelated RE ions on interfacing aggregates. The size of the finally obtained UCNs is confined by the restricted supply of RE ions. As revealed by transmission electron microscopy (TEM), UCNs (3 h growth) show good monodispersity with the average size of $\sim$6.3 $\pm$ 0.3 nm (100 samples) (Fig. S3b in the ESI†). In agreement with our hypothesis, prolonged reaction (8 h) doesn't significantly increase the UCN size ($\sim$6.6 $\pm$ 0.3 nm, 100 samples) further (Fig. 2a). The XRD peaks of the obtained nanoparticles are in accordance with that from α-UCNs (Fig. S4a in the ESI†). In summary, because faciliated nucleation at ambient temperature and growth at high temperature with restricted supply of RE ions are separated in this synthesis, the resulting UCNs are small and uniform.

As shown in Fig. 2b and c, when sodium acrylate (3 carbon fatty acid) or sodium oatanoate (8 carbon fatty acid) is used as

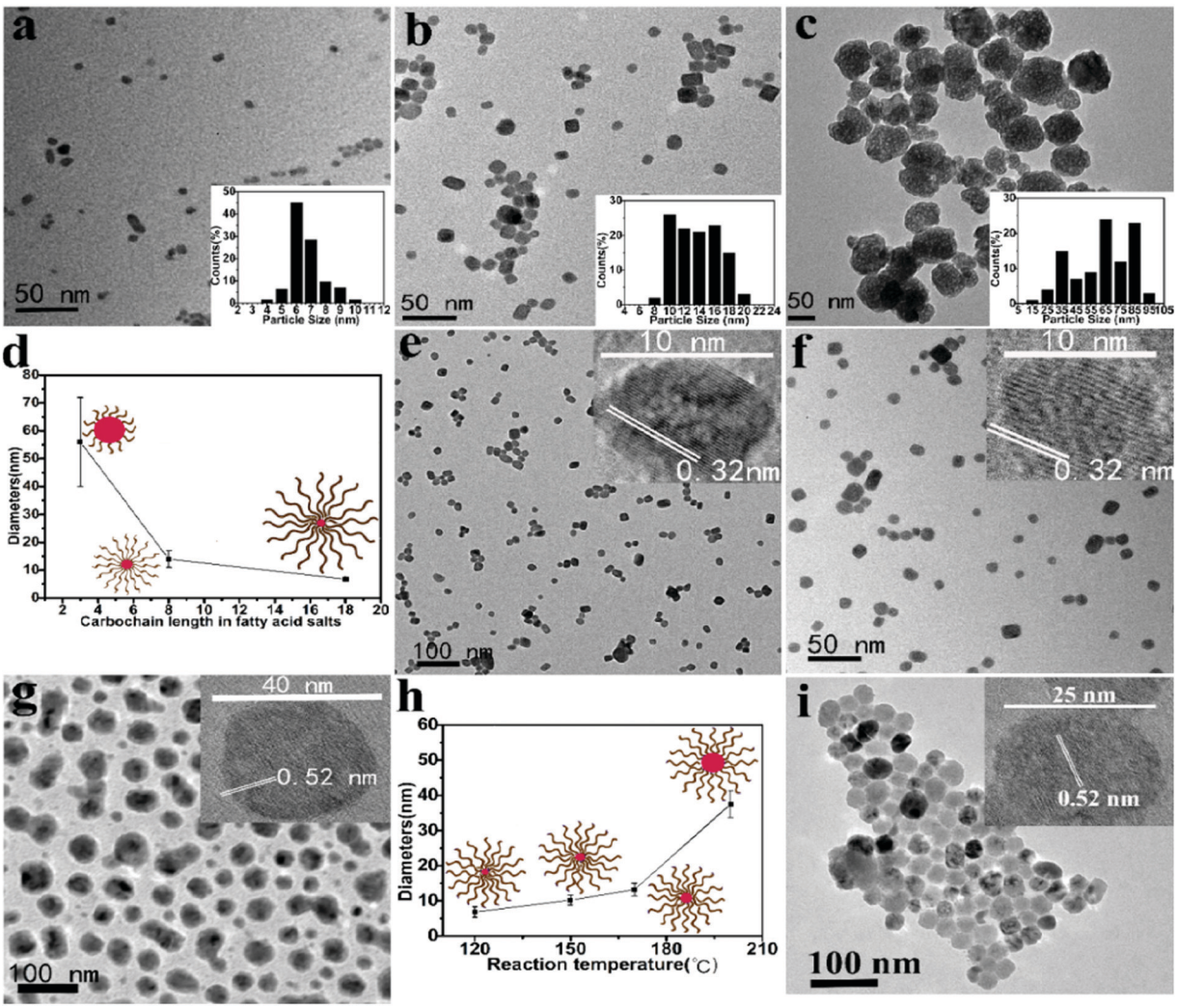

Fig. 2 TEM images of the UCNs synthesized using (a) sodium oleate, (b) sodium oatanoate and (c) sodium acrylate under 120 °C hydrothermal conditions for 8 h. Insets show the size distribution. (d) UCN size *versus* the carbochain length of the used fatty acid. TEM images of the UCNs synthesized using sodium oleate under (e) 150 °C, (f) 170 °C and (g) 200 °C for 8 h. Insets present HRTEM images. (h) UCN size *versus* the reaction temperature. (i) TEM image of the prepared UCNs with the F^-/Y^{3+} molar ratio of 32 (7 h reaction at 150 °C).

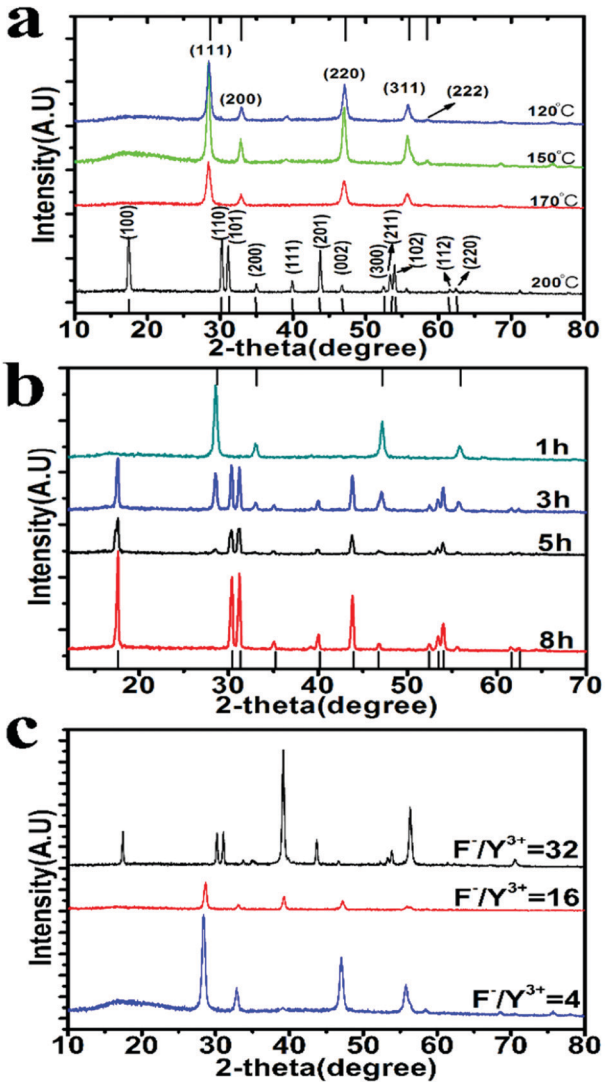

Fig. 3 (a) XRD spectra of the UCNs obtained at different reaction temperatures for 8 h. PDF (no. 01-077-2042) of cubic α-phase and PDF (no. 00-016-0334) of hexagonal β-phase $NaYF_4$ are indicated at the top and bottom axis, respectively. (b) XRD spectra of the UCNs prepared using different reaction durations at 200 °C. (c) XRD spectra of the UCNs prepared at 150 °C for 7 h with different F^- to Y^{3+} molar ratios.

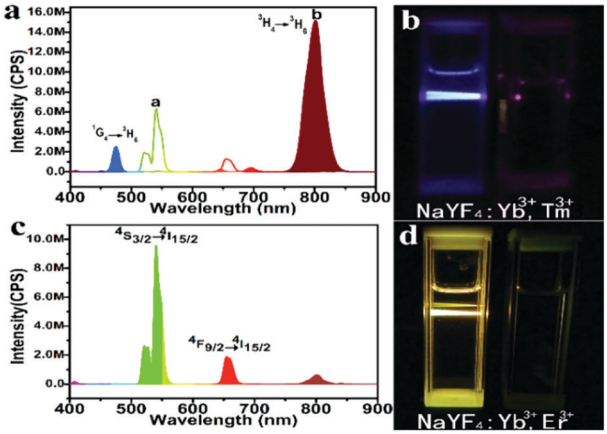

Fig. 4 (a) UC PL spectra of the prepared β-phase $NaYF_4$:Yb^{3+},Tm^{3+} nanocrystals (1 mg mL^{-1}) and the commercial upconversion $NaYF_4$:Yb^{3+},Er^{3+} nanocrystals (Sigma) (1mg mL^{-1}) under 980 nm laser excitation with 0.5 W. (b) The photographic image of the β-phase nanocrystal solution without and with laser excitation at 980 nm. (c) UC PL spectra of the prepared $NaYF_4$:Yb^{3+},Er^{3+} nanocrystals under laser excitation at 980 nm. (d) The photographic image of β-phase $NaYF_4$:Yb^{3+},Er^{3+} nanocrystal solutions without and with laser excitation at 980 nm.

the chelator of RE ions and stabilizer of UCNs, the same synthesis produces much larger α-UCNs with wide size distribution (~56.2 ± 16.3 nm, 100 samples; ~15.5 ± 1.5 nm, 100 samples). This is because these two fatty acids within (RE) ions cannot form aggregates (Fig. S5a and b in the ESI†) and therefore are not able to assist nucleation at ambient temperature (TEM not shown). The UCNs obtained from sodium oatanoate are relatively small conceivably because the fatty acid chains on the UCN surface limit the growth rate by restricting the diffusion of RE ions in the solution to the nucleation core. As evidenced by Fig. 2d, we propose that the size of UCNs can be controlled by the chain length of the used fatty acid.

The small-sized UCNs are particularly attractive for *in vivo* applications. Our α-phase $NaYF_4$:Yb^{3+},Tm^{3+} nanocrystal is the smallest UCN using $NaYF_4$ as the host material.[19–21] Thus far, the demonstration of ultrasmall UCNs is still limited, and they are all synthesized in an organic medium at high temperature (>300 °C) with moderate production yield.[15,24–27] Using our methods, a high yield of ~86% with a very low concentration of Y^{3+} (6.4 mM which is an order lower than typically needed) is obtained.[15]

The size of UCNs increases with the increasing reaction temperature (Fig. 2e–g) presumably because a higher temperature makes the chelated Y^{3+} ions become more mobile in the aggregates. The characteristic lattice spacing resolved by high-resolution TEM (HRTEM) indicates that UCNs obtained at 120, 150, and 170 °C are α-phase while 200 °C produces β-UCNs.

XRD characterization also confirms their phase identity (Fig. 3a). Under 200 °C, 1 h reaction yields α-UCNs only; 3 h reaction gives a mixture of α- and β-UCNs; 5 h and above produce only β-UCNs (Fig. 3b). As expected, increasing temperature and reaction time favors the transition from α to β phase. Notably, α to β phase transition doesn't occur under the same conditions when sodium acrylate or sodium oatanoate are used (Fig. S4b in the ESI†). This implies that aggregate-assisted nucleation is more thermodynamically stable and favors the phase transition.

The previous studies have demonstrated that increasing the F^- to Y^{3+} ratio promotes α to β phase transition,[20] because excessive F^- ions passivate the dangling bonds on UCN thereby reducing the surface energy of the nanoparticle. With F^- to Y^{3+} ratio of 32 (Y^{3+} reduced from 26.4 mM to 6.6 mM while F^- being increased from 108 mM to 216 mM), the reaction time for phase transition at 200 °C is largely decreased from 5 h to 1 h (Fig. S4c in the ESI†). But the reaction at such high temperature leads to heterogeneous distribution of the produced nanoparticles.

Fig. 3c demonstrates that α to β transformation can occur at 150 °C with F^- to Y^{3+} ratio of 32 when the reaction time is increased to 7 h. As uncovered by TEM (Fig. 2i), the obtained

β-UCNs have uniform size distribution (25.5 ± 0.3 nm, 100 samples). The size uniformity is attributable to the low reaction temperature as well as aggregate-controlled growth by adjusting local precursor supersaturation. TEM imaging shows that the formed β-UCNs are surrounded by aggregates (Fig. S4d in the ESI†). Reducing the F^- to Y^{3+} ratio fails to produce β-UCNs under the same conditions (Fig. 3c). The previous synthesis methods for β-UCNs all require much higher temperature.[20–29] And they often need long reaction time and sometimes produce large-sized particles.[22–29]

Under 980 nm laser excitation, the upconversion photoluminescence (UC PL) spectra of the β-phase $NaYF_4$:Yb^{3+},Tm^{3+} nanocrystals prepared at 150 °C exhibit two prominent peaks around 475 nm and 800 nm, which resulted from $^1G_4 \rightarrow {}^3H_6$ and $^3H_4 \rightarrow {}^3H_6$ transitions of Tm^{3+} ions, respectively (Fig. 4a). Under 0.5 W laser, the nanocrystal solution (5 mg mL^{-1}) appears bright blue (Fig. 4b), indicating its high quantum yield. Subjected to the same excitation at 980 nm, the emission peak of our UCNs at NIR (800 nm) is ~2.3 times that from a commercial green UCN (Sigma-Aldrich, $NaYF_4$:Yb^{3+},Er^{3+}).

To demonstrate the versatility of our approach, we synthesized another class of upconversion nanocrystals, namely, $NaYF_4$:Yb^{3+},Er^{3+}. Fig. S6a and b (ESI†) present the representative TEM images of α-phase and β-phase $NaYF_4$:Yb^{3+},Er^{3+} nanocrystals, respectively. The strong emission around 542 nm and 654 nm from the β-phase UCN are originated from $^4S_{3/2} \rightarrow {}^4I_{15/2}$ and $^4F_{9/2} \rightarrow {}^4I_{15/2}$ transition of Er^{3+} (Fig. 4c and d). Weak acid treatment to remove oleate and the conjugating poly (acrylic acid) (PAA) on the UCN under solvothermal conditions renders the nanocrystals water soluble for bio-applications (Fig. 1). Using Fourier-transform infrared spectroscopy (FTIR), the success of PAA attachment is confirmed by the vibration peak (3468 cm^{-1}) of C–H bond and the vibration peak (1642 cm^{-1}) of C═O from PAA (Fig. S7 in the ESI†).

Conclusions

In summary, a new green method to synthesize upconversion nanocrystals (UCNs) with high production yield at low temperature has been demonstrated. Fatty acids are used as the chelator for rare earth ions and stabilizer of UCNs, allowing the synthesis to occur under aqueous conditions. Aggregates formed by fatty acids facilitate the nucleation at low temperature by adjusting the local precursor supersaturation. And such a synthesis allows separation of nucleation and growth, leading to formation of ultrasmall α-phase UCNs with uniform size distribution (~6.3 nm). The particle size can be tuned by choosing fatty acids with different carbon chain lengths. And at moderately increased temperature, α to β phase transition can occur producing bright NIR-emitting UCNs. In principle, other aggeregates forming molecules other than fatty acids may also be used and the same strategy may also be applied for high quality synthesis of other nanocrystals.

Conflicts of interest

There are no conflicts to declare.

Acknowledgements

This work was financially supported by an AcRF tier 2 grant (MOE2017-T2-2-005) from the Ministry of Education (Singapore). We sincerely appreciate the National Natural Science Foundation of China for the financial support (81573388). This work was supported by "Qing Lan Project of Jiangsu Province" and "Six Talent Peaks Project of Jiangsu Province (YY-032)". This work was also supported by the Open Project Program of Jiangsu Key Laboratory for Pharmacology and Safety Evaluation of Chinese Materia Medica (No. JKLPSE201805).

Notes and references

1 D. Vennerberg and Z. Lin, *Sci. Adv. Mater.*, 2011, **3**, 26–40.
2 H. Wen, H. Zhu, X. Chen, T. F. Hung, B. Wang, G. Zhu, S. F. Yu and F. Wang, *Angew. Chem., Int. Ed.*, 2013, **52**, 13419–13423.
3 H. Wen, H. Zhu, X. Chen, T. F. Hung, B. Wang, G. Zhu, S. F. Yu and F. Wang, *Angew. Chem., Int. Ed.*, 2013, **125**, 13661–13665.
4 D. K. Chatterjee, M. K. Gnanasammandhan and Y. Zhang, *Small*, 2010, **6**, 2781–2795.
5 (*a*) A. D. Ostrowski, E. M. Chan, D. J. Gargas, E. M. Katz, G. Han, P. J. Schuck, D. J. Milliron and B. E. Cohen, *ACS Nano*, 2012, **6**, 2686–2692; (*b*) T. Rinkel, J. Nordmann, A. N. Raj and M. Haase, *Nanoscale*, 2014, **6**, 14523–14530.
6 (*a*) C. Zhang, H. P. Zhou, L. Y. Liao, W. Feng, W. Sun, Z. X. Li, C. H. Xu, C. J. Fang, L. D. Sun and Y. W. Zhang, *Adv. Mater.*, 2010, **22**, 633–637; (*b*) R. Deng, F. Qin, R. Chen, W. Huang, M. Hong and X. Liu, *Nat. Nanotechnol.*, 2015, **10**, 237–242.
7 (*a*) H. H. Gorris and O. S. Wolfbeis, *Angew. Chem., Int. Ed.*, 2013, **52**, 3584–3600; (*b*) J. Lee, P. W. Bisso, R. L. Srinivas, J. J. Kim, A. J. Swiston and P. S. Doyle, *Nat. Mater.*, 2014, **13**, 524–529.
8 Y. Lu, J. Lu, J. Zhao, J. Cusido, F. M. Raymo, J. Yuan, S. Yang, R. C. Leif, Y. Huo, J. A. Piper, J. Paul Robinson, E. M. Goldys and D. Jin, *Nat. Commun.*, 2014, **5**, 3741.
9 (*a*) P. Zhang, P. Steelant, M. Kumar and M. Scholfield, *J. Am. Chem. Soc.*, 2007, **129**, 4526–4527; (*b*) F. Wang, D. Banerjee, Y. Liu, X. Chen and X. Liu, *Analyst*, 2010, **135**, 1839–1854.
10 (*a*) F. Wang and X. G. Liu, *J. Am. Chem. Soc.*, 2008, **130**, 5642–5643; (*b*) S. W. Wu, G. Han, D. J. Milliron, S. Aloni, V. Altoe, D. V. Talapin, B. E. Cohen and P. J. Schuck, *Proc. Natl. Acad. Sci. U. S. A.*, 2009, **106**, 10917–10921; (*c*) M. X. Yu, F. Y. Li, Z. G. Chen, H. Hu, C. Zhan and C. H. Huang, *Anal. Chem.*, 2009, **81**, 930.
11 (*a*) G. Jalani, R. Naccache, D. H. Rosenzweig, L. Haglund, F. Vetrone and M. Cerruti, *J. Am. Chem. Soc.*, 2016, **138**(3), 1078–1083; (*b*) L. Q. Xiong, Z. G. Chen, Q. W. Tian, T. Y. Cao, C. J. Xu and F. Y. Li, *Anal. Chem.*, 2009, **81**, 8687.
12 J. C. Boyer, M. P. Manseau, J. L. Murray and F. C. J. M. van Veggel, *Langmuir*, 2010, **26**, 1157.
13 M. Nyk, R. Kumar, T. Y. Ohulchanskyy, E. J. Bergey and P. N. Prasad, *Nano Lett.*, 2008, **8**, 3834–3838.
14 H. S. Choi, W. Liu, P. Misra, E. Tanaka, J. P. Zimmer, B. I. Ipe, M. G. Bawendi and J. V. Frangioni, *Nat. Biotechnol.*, 2007, **25**, 1165.

15 G. Y. Chen, H. L. Qiu, P. N. Prasad and X. Y. Chen, *Chem. Rev.*, 2014, **114**, 5161–5214.
16 A. N. Raj, T. Rinkel and M. Haase, *Chem. Mater.*, 2014, **26**, 5689–5694.
17 N. J. J. Johnson, W. Oakden, G. J. Stanisz, R. S. Prosser and F. C. J. M. van Veggel, *Chem. Mater.*, 2011, **23**, 3714–3722.
18 B. Voß, J. Nordmann, A. Uhl, R. Komban and M. Haase, *Nanoscale*, 2013, **5**, 806–812.
19 Q. Liu, Y. Sun, T. S. Yang, W. Feng, C. G. Li and F. Y. Li, *J. Am. Chem. Soc.*, 2011, **133**, 17122–17125.
20 T. Rinkel, A. N. Raj, S. Dîhnen and M. Haase, *Angew. Chem., Int. Ed.*, 2016, **55**, 1164–1167.
21 G. Y. Chen, T. Y. Ohulchanskyy, R. Kumar, H. Ågren and P. N. Prasad, *ACS Nano*, 2010, **4**(6), 3163–3168.
22 (*a*) M. Sindoro, N. Yanai, A. Y. Jee and S. Granick, *Acc. Chem. Res.*, 2014, **47**, 459–469; (*b*) X. G. Wang, Q. Cheng, Y. Yu and X. Z. Zhang, *Angew. Chem.*, 2018, **130**, 7962–7966.
23 L. Y. Pan, M. He, J. B. Ma, W. Tang, G. Gao, R. He, H. C. Su and D. X. Cui, *Theranostics*, 2013, **3**(3), 210–222.
24 C. Burda, X. B. Chen, R. Narayanan and M. A. El-Sayed, *Chem. Rev.*, 2005, **105**, 1025–1102.
25 (*a*) B. L. Cushing, V. L. Kolesnichenko and C. J. O'Connor, *Chem. Rev.*, 2004, **104**, 3893–3946; (*b*) J. C. Boyer, L. A. Cuccia and J. A. Capobianco, *Nano Lett.*, 2007, **7**, 847–852.
26 X. Liang, X. Wang, J. Zhuang, Q. Peng and Y. D. Li, *Adv. Funct. Mater.*, 2007, **17**, 2757–2765.
27 F. Wang, Y. Han, C. S. Lim, Y. Lu, J. Wang, J. Xu, H. Chen, C. Zhang, M. Hong and X. Liu, *Nature*, 2010, **463**, 1061–1065.
28 D. J. Gargas, E. M. Chan, A. D. Ostrowski, S. Aloni, M. V. P. Altoe, E. S. Barnard, B. Sanii, J. J. Urban, D. J. Milliron, B. E. Cohen and P. J. Schuck, *Nat. Nanotechnol.*, 2014, **9**, 300–305.
29 F. Shi and Y. Zhao, *J. Mater. Chem. C*, 2014, **2**, 2198–2203.
30 S. H. Feng and R. R. Xu, *Acc. Chem. Res.*, 2001, **34**, 239–247.
31 X. Wang and Y. Li, *Chem. Commun.*, 2007, 2901–2910.